

Is soft physics entropy driven?

Helen Caines¹

Yale University, Physics Department, New Haven, CT 06520

Received: date / Revised version: date

Abstract. The soft physics, $p_T < 2$ GeV/c, observables at both RHIC and the SPS have now been mapped out in quite specific detail. From these results there is mounting evidence that this regime is primarily driven by the multiplicity per unit rapidity, $dN_{ch}/d\eta$. This suggests that the entropy of the system alone is the underlying driving force for many of the global observables measured in heavy-ion collisions. That this is the case and there is an apparent independence on collision energy is surprising. I present the evidence for this multiplicity scaling and use it to make some extremely naive predictions for the soft sector results at the LHC.

PACS. PACS-key describing text of that key – PACS-key describing text of that key

1 Introduction

Back in 1965, Hagedorn postulated that the hadronic mass spectrum grows exponentially with mass [1]. Since 1965, more than 3200 additional resonance states have been identified and these results seem to confirm Hagedorn's hypothesis. The exponential growth means that adding more energy to a system merely produces more particles, resulting in a limiting temperature, $T_0 \sim 160$ MeV for a hadron gas. Interestingly this value of T_0 is very close to the limiting chemical freeze-out temperature, T_{ch} , calculated via statistical production models, from data as a function of $\sqrt{s_{NN}}$, (see Fig. 1 [2]). We know that entropy is related to temperature and energy via $T\Delta S = \Delta E$. If the calculations are correct and chemical freeze-out temperatures reach a maximal value then, as the collision energy increases, the entropy of the system must also increase.

Even before Hagedorn's work Landau and Fermi related pion production in high energy collisions to the entropy produced [3,4]. I will try and reproduce the main points of their arguments here. The energy density, ϵ , available for particle creation in a collision is

$$\epsilon = \frac{E}{V} = \frac{(\sqrt{s_{NN}} - 2m_N)\sqrt{s_{NN}}}{2m_NV_0} \quad (1)$$

where: V_0 is the volume and m_N is the mass of the nucleon. If you assume that the entropy is produced early in the collision, that the source is thermalized and that it expands adiabatically, the entropy, S , can be related to ϵ via the equation of state (EoS). Thus, entropy and the produced particle multiplicity are correlated.

A simple example of such a correlation can be derived using the EoS of a system of massless pions which emits

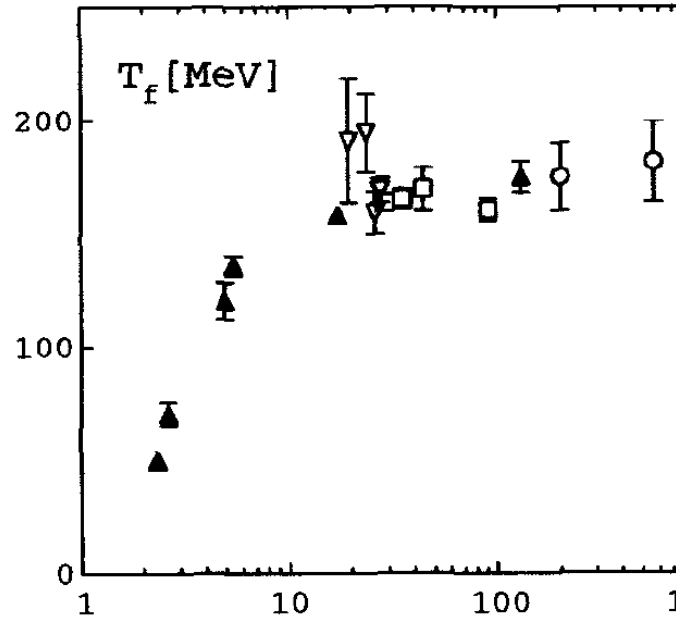


Fig. 1. The calculated T_{ch} as a function of collision energy, for e^+e^- (squares), $p-p$ (open triangles) $p\bar{p}$ (circles) and A-A (closed triangles). Data from [2].

as a blackbody. In this case, $p = \epsilon/3$ and $\epsilon = T^4$. Thus

$$s = S/V \quad (2)$$

$$Ts \sim \epsilon + p \quad (3)$$

$$s \sim \epsilon^{3/4} \quad (4)$$

and

$$S \sim V((\sqrt{s_{NN}} - 2m_N)\sqrt{s_{NN}})^{3/4} \quad (5)$$

$$\sim \frac{N_{part}(\sqrt{s_{NN}} - 2m_N)^{3/4}}{\sqrt{s_{NN}}^{1/4}} \quad (6)$$

The $\sqrt{s_{NN}}$ dependence of the entropy in Eqn. 6 is the same as that derived by Fermi [4] and S/V is called the Fermi energy, F . If these arguments hold, a plot of the measured entropy density, or mean multiplicity per participant nucleon, versus F , calculated from the right-hand side of Eqn. 6 should result in a linear correlation. Such a correlation can be seen in Fig. 2, taken from [5]. In this plot, although only the mean pion multiplicities are used, this is a good approximation to the total multiplicity. It can be seen that the multiplicity per participant of the p - p collision data, open circles, is indeed proportional to F . The A-A data seem to depart from this curve at the top AGS energy. This apparent increase in entropy in higher energy collisions was first observed by 1995 and interpreted as evidence of a transition to quark degrees of freedom resulting in a different EoS [6].

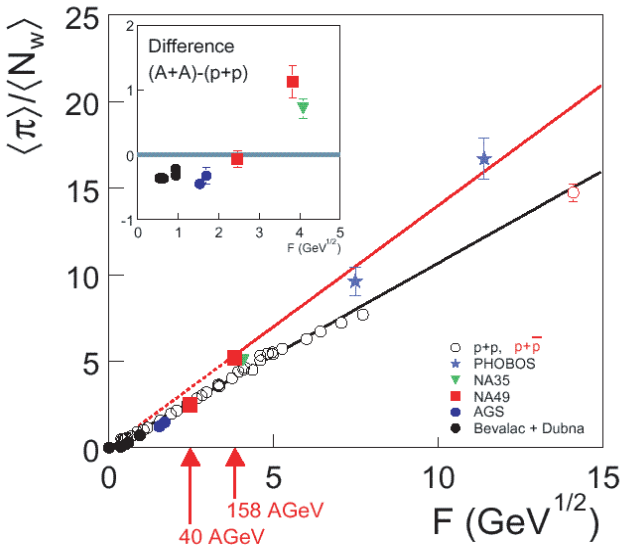


Fig. 2. Entropy per participant versus the Fermi energy variable (only pion multiplicities were used) for various collision energies [5].

Since there appears to be evidence that particle multiplicity and entropy are correlated over a range of collision energies, it is interesting to see if entropy, e.g. multiplicity, can be used to determine unique scalings for other bulk physics measurements. The rest of this paper discusses femtoscopic measurements, elliptic flow and strangeness yields and uses entropy scalings to make naive predictions for these observables at the LHC.

2 Femtoscopy

Femtoscopic measurements examine space-momentum correlations and allow, in a model dependent fashion, for the extraction of source sizes. For more details on these techniques see elsewhere [8]. Detailed measurements have been made, especially looking into identical pion correlations. While the radii hover around 5 fm, when the results are plotted as a function of $\sqrt{s_{NN}}$, see Fig. 3 left panel [9], no clear trends appear. However, if, as in Fig. 3 right panel, the same measurements are now plotted as a function of $(dN_{ch}/d\eta)^{1/3}$ a clear scaling is observed for R_{long} and R_{side} . The applicability to R_{out} is less clear. This lack of scaling for R_{out} might have an explanation via the fact that this HBT variable consists of a convolution of terms containing length and time scales. R_{long} and R_{side} are, on the other hand, pure length measurements. The deviations in R_{out} might therefore be signatures of differing timescales for the collisions. It should be noted that while the right panel of Fig. 3 is for $\langle k_T \rangle = 400$ MeV and 390 MeV for RHIC and SPS respectively. As good a scaling is observed if other $\langle k_T \rangle$ ranges are selected. The non-monotonic behavior seen in the left panel of Fig. 3 for $\sqrt{s_{NN}} < 5$ GeV makes it obvious that the $dN_{ch}/d\eta$ scaling breaks down at very low collision energies. It has been pointed out, by the CERES collaboration, that this is probably due to the dominance of baryons at lower $\sqrt{s_{NN}}$ [10].

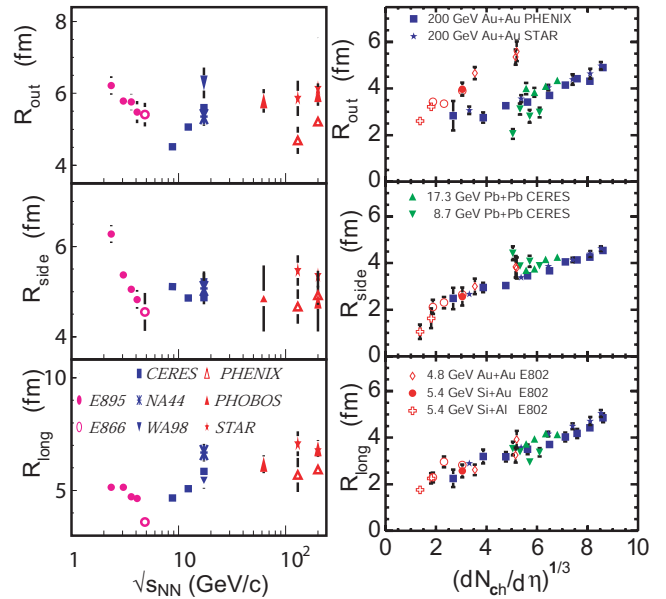


Fig. 3. Left panel) World dataset of published HBT radii from central Au+Au (Pb+Pb) collisions versus collision energy. Compilation from [7]. Right panel) The same measurements as in the left panel but as a function of $(dN_{ch}/d\eta)^{1/3}$

3 Elliptic Flow

Peripheral and low energy collisions are likely to produce systems with incomplete thermalization. Since re-scattering of the particles is rare, in this low density limit regime, little change occurs, on average, to the initial momentum distributions. The measured elliptic flow, v_2 , is therefore proportional to the initial state eccentricity, ϵ , as determined via Glauber calculations, and the space density of the initial particles. The latter determining the scattering probability which must be finite so that the initial spatial anisotropy can be converted into a measurable momentum anisotropy. Thus,

$$v_2 \propto \frac{1}{Area} \frac{dN}{dy} \epsilon \quad (7)$$

$$\epsilon = \frac{(R_x^2 - R_y^2)}{(R_x^3 + R_y^3)} \quad (8)$$

where R_x and R_y are the major and minor axes of the overlap ellipse of the colliding nuclei in the transverse plane. From Eqn. 8 it can be seen that in the most central A-A collisions ϵ , and hence v_2 , tends towards zero. In the Cu-Cu data however there remains a significant measured v_2 component in the most central events, Fig. 4, [11].

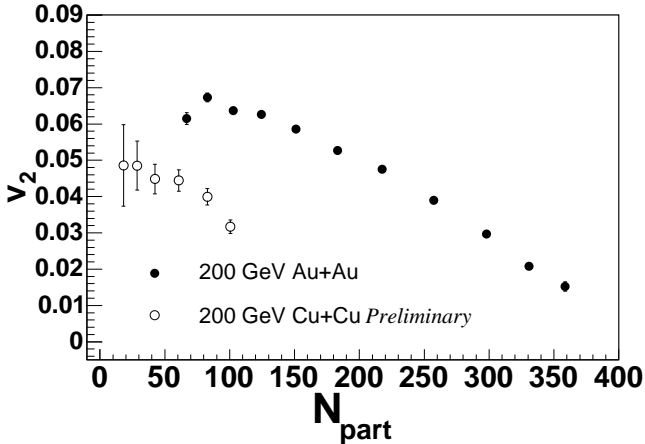


Fig. 4. Elliptic flow, v_2 , measured near mid-rapidity as a function of N_{part} for Cu-Cu (open symbols) and Au-Au (closed symbols) collisions at $\sqrt{s_{NN}} = 200$ GeV. Only statistical errors are shown, taken from [11].

Also when, for a given number of participants, N_{part} , v_2/ϵ measurements in Cu-Cu are contrasted to similarly scaled Au-Au results, they are not compatible. This suggests that the low density limit concept is not applicable to the data [12]. Since the Cu-Cu results are above those of the Au-Au at a given N_{part} , other conclusions could be drawn from these data. These are that either the Cu-Cu system is more efficient at translating spatial anisotropies into v_2 signals or there are significant non-flow effects in

the Cu-Cu data that create these large momentum asymmetries. An alternative explanation can however be postulated by examining the initial state eccentricity calculation. As stated above this is traditionally defined as an average eccentricity calculated from the participant nucleon distributions relative to the reaction plane for each centrality class via Glauber calculations. This method leads to two possible errors: firstly event-by-event fluctuations are averaged to zero and secondly, while the minor axis of the participant distribution is along the impact parameter vector on average for any given event this will not generally be the case. In events with a small number of participants these two effects can cause a significant error in the eccentricity calculations [11]. The PHOBOS collaboration have therefore proposed a new technique for calculating the eccentricity, called ϵ_{part} , which takes these effects into account [12]. When the v_2/ϵ_{part} ratio is then plotted versus the mid-rapidity area density of produced particles, Fig. 5, good agreement is now observed between the two collision systems. Also shown in this plot are results from $\sqrt{s_{NN}} = 17$ and 4 GeV and a common scaling seems to emerge. This suggests that v_2 depends solely on the initial area density achieved in the collision over two orders of magnitude in collision energy. Note that a linear dependence on dN/dy or entropy has emerged.

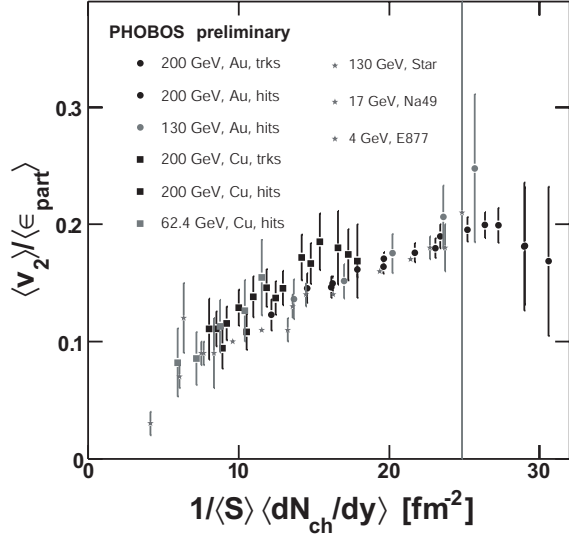


Fig. 5. v_2 per average participant eccentricity as a function of mid-rapidity area density. Data are from RHIC Au-Au collisions at $\sqrt{s_{NN}} = 130$ and 200 GeV and Cu-Cu collisions at $\sqrt{s_{NN}} = 62.4$ and 200 GeV as well as SPS $\sqrt{s_{NN}} = 17$ GeV and AGS $\sqrt{s_{NN}} = 4$ GeV collisions [11].

4 Strange particle production

A lack of phase space in p - p collisions is predicted to result in strangeness production being suppressed [13]. The magnitude of this suppression decreases with increasing $\sqrt{s_{NN}}$

and with the volume of the medium produced. Since the collision volume is linearly proportional to N_{part} , it is also predicted that the strangeness production volume follows such a linear scaling. The calculations also show that the p - p suppression increases with the particle's strangeness content. When the system becomes sufficiently large, the phase space restrictions are removed and strangeness can be produced freely. For these types of collisions, the ratio of strangeness yield to N_{part} is therefore a constant as a function of centrality.

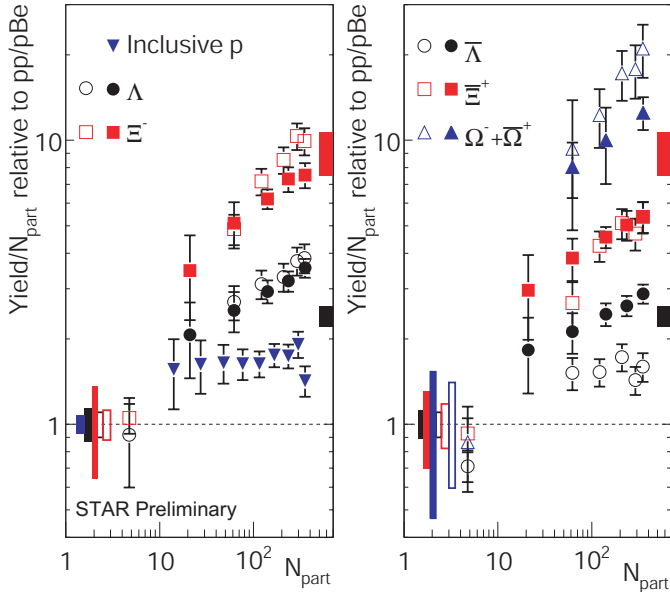


Fig. 6. Yield per participant relative to the yield per participant in p - p collisions as a function of N_{part} . Solid symbols are for Au-Au collisions at $\sqrt{s_{NN}} = 200$ GeV, and the open symbols are measured by NA57 from Pb-Pb at $\sqrt{s_{NN}} = 17.3$ GeV. The boxes represent the combined statistical and systematical uncertainties in the p - p and p -Be data. The error bars on the data points represent those from the heavy-ion measurement. The boxes on the right axes mark the predictions from a model using a Grand Canonical formalism described in [13].

It can be seen in Fig. 6 that in Au-Au collisions at $\sqrt{s_{NN}} = 200$ GeV, although the predicted strangeness ordering of the p - p suppression is observed the yields per participant are not constant. Further, the magnitude of the suppression for a given strange baryon is the same in $\sqrt{s_{NN}} = 200$ GeV collisions as at the SPS in $\sqrt{s_{NN}} = 17.3$ GeV collisions [14, 15]. Both of these results are counter to the predictions. Calculations using statistical models applied to the STAR data indicate that γ_s , the strangeness saturation factor, is unity in central collisions, e.g. that there is no suppression in the most central data [16]. This suggests that the relevant volume for strangeness production is not linearly proportional to N_{part} and hence not purely related to the initial collision overlap volume. Therefore some other scaling must be sought.

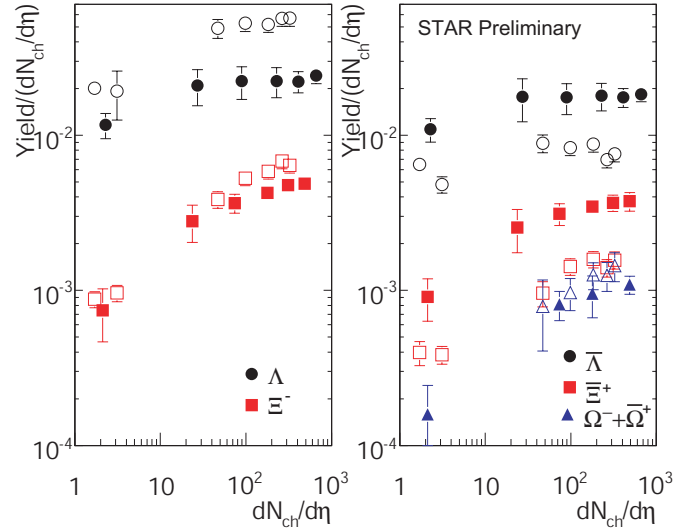


Fig. 7. Yield per $dN_{ch}/d\eta$ as a function of $dN_{ch}/d\eta$ for strange (anti)baryons. Solid symbols are for Au-Au collisions at $\sqrt{s_{NN}} = 200$ GeV, and the open symbols are measured by NA57 from Pb-Pb at $\sqrt{s_{NN}} = 17.3$ GeV [15].

Figure 7 shows the yield per $dN_{ch}/d\eta$ for Λ , $\bar{\Lambda}$, Ξ^- , $\bar{\Xi}^+$, and $\Omega^- + \bar{\Omega}^+$ for RHIC and the SPS Pb-Pb collisions using data taken from [14, 15]. When plotted in this way the yield/ $dN_{ch}/d\eta$ appears constant for the more central data suggesting that an entropy measure is more closely correlated to the strangeness production volume than the number of participants.

5 LHC predictions

As shown in Fig. 2, it appears that the EoS for heavy-ion collisions is different to that in p - p . We also expect it to be much more complicated than that derived earlier for a gas of massless pions. There can still be a functional relationship between entropy and $\sqrt{s_{NN}}$. In Fig. 8, taken from [17], measurements of the mid-rapidity $dN_{ch}/d\eta$ per participant pair are shown as a function of collision energy, note the log scale on the abscissa. This plot clearly shows a linear scaling of $N_{ch}/d\eta$ per participant pair with $\log(\sqrt{s_{NN}})$ again over several orders of magnitude. This dramatic scaling allows an estimation of the change in entropy as a function of beam energy to be made.

Making a leap of faith, one can naively extend this scaling to the LHC energy regime of 5.5 TeV, as performed in [9], and shown by the solid line in Fig. 8. Such an extrapolation leads to the expectation that mid-rapidity multiplicities will be as little as 60% higher than they are at RHIC, e.g. the mid-rapidity yield will be of order 1200 charged particles. Armed with this “knowledge” of the expected LHC multiplicity/entropy one can continue to make simple extrapolations. I use the scalings with entropy for the other bulk physics measurements discussed above. Thus predictions for the HBT radii, elliptic flow and strangeness yields are obtained.

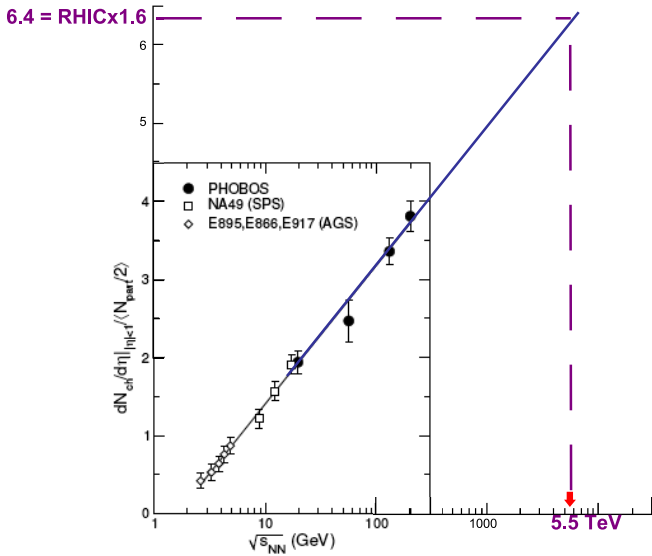


Fig. 8. The multiplicity density per participant pair measured in Au-Au and Pb-Pb collisions at AGS, SPS, and RHIC. Taken from [17], and naively extrapolated to LHC energies in [9].

The femtoscopic radii were shown to depend primarily on the cube root of the mid-rapidity event multiplicity. Thus the combination of Figures 3 and 8 suggests that HBT measurements in central collisions at LHC will be $\sim 17\%$ higher than at RHIC ($(1.6)^{1/3} = 1.17$). Precise expectations for R_{out} at the LHC are, admittedly, less certain, as the former does not scale exactly with multiplicity (Fig. 3).

To make a prediction for the value of elliptic flow in the most central collisions one needs a calculation of the mid-rapidity transverse area. For Pb-Pb collisions Glauber calculations show an initial RMS transverse radius of ~ 2.8 fm and hence a mean particle area density of $\sim 50 \text{ fm}^{-2}$. Using a straight line extrapolation from the data shown in Fig. 5, one would predict $v_2/\epsilon_{part} = 0.35$. However, it should be remembered that the proportionality of elliptic flow to the mean transverse area density is only predicted to hold in the low particle density limit. It is hard to believe that central Au-Au or Pb-Pb collisions produce low area densities and there is much evidence that the re-scattering rate is high at RHIC, for instance the large amount of radial flow [18,19] and the significant regeneration of resonances after chemical freeze-out [20]. Taking these, and other, RHIC results into consideration it is more likely that central RHIC/LHC collisions are hydrodynamical in behavior. If this is the case, v_2/ϵ will be a constant, assuming the same EoS holds at RHIC and the LHC. If one takes a second look at Fig. 5 it is possible that the higher centrality Au-Au data points are pulling away from a straight line fit towards a plateau. Therefore instead of LHC collisions increasing further the elliptic flow to eccentricity ratio is likely to stay constant at $v_2/\epsilon = 0.2$.

Although the strangeness yields cannot be directly extracted from Fig. 7, an estimate can still be made for the LHC regime. From Fig. 7 it can be seen that whereas the $\bar{\Lambda}/\Lambda$ ratio at the SPS is ~ 0.1 , at RHIC the mid-rapidity anti-baryon to baryon ratio is very close to unity. It can also be seen that the SPS strangeness yields per $N_{ch}/d\eta$ for the (anti) Λ and (anti) Ξ frame those measured at RHIC. These results suggest therefore that the LHC net-baryon number will be essentially zero and that the yield per charged particle at mid-rapidity will be the same as that measured at $\sqrt{s_{NN}} = 200$ GeV. Given that the entropy extrapolations predict an $\sim 60\%$ increase in charged particle production one can therefore expect a similar increase in the strange baryon yields when going from RHIC to the LHC. Thus, $dN_{\Lambda}/dy = dN_{\bar{\Lambda}}/dy = \sim 20 - 30$, $dN_{\Xi^-}/dy = dN_{\bar{\Xi}^+}/dy = \sim 4 - 6$ and $dN_{\Omega^- + \bar{\Omega}^+}/dy = \sim 0.5-1$ in the most central events.

6 Summary

In summary, from simple arguments it can be shown that produced particle multiplicities are strongly correlated to the entropy of the system and that a limiting temperature is reached if the matter being probed is hadronic. Further, when heavy-ions are collided at high energies, the trend of this entropy measure versus the Fermi energy is different to that in $p-p$ and low $\sqrt{s_{NN}}$ heavy-ion collisions.

Evidence is mounting that many observables from the soft-sector are determined primarily by total multiplicity, i.e. entropy. The HBT radii, properly-scaled elliptic flow, and strangeness yields, all appear to show universal multiplicity scalings. This implies that bulk observables are dominated by entropy-driven factors. There is also much evidence that these high-energy collisions produce a new phase of matter that consists of interacting quarks and gluons. That this highly non-trivial source apparently produces signatures, in the soft momentum sector, with dependencies only on multiplicity and not reaction energy is very intriguing.

These multiplicity scalings can then be used to make naive predictions for some soft sector results at the LHC. However, anything can, of course occur when this new regime is probed as novel physics could be probed. However, any significant deviation from these apparent universal multiplicity scalings would be extremely interesting. Whatever the outcome the first results from CERN, now only just over a year away, are eagerly awaited.

References

1. R. Hagedron, Nuovo Cim. Suppl. **3** (1965) 147.
2. H. Satz, Nucl. Phys. **A715** (2003) 3c.
3. L.D. Landau, Izv. Akad. Nauk SSSR, Ser. Fiz **17**, (1953) 51.
4. E. Fermi, Prog. Theor. Phys. **5** (1950) 570.

5. P. Seyboth, Proceedings of the 17th Winter Workshop (2001). <http://na49info.cern.ch/cgi-bin/wwwd-util/NA49/NOTE?265>.
6. M. Gazdicki and D. Rörich, Z. Phys. C **65** (1995) 215.
7. M.A. Lisa, S. Pratt, R. Soltz, and U. Wiedemann, Ann. Rev. Nucl. Part. Sci. **55** (2005) 311.
8. M. Lisa these proceedings.
9. M. Lisa nucl-ex/0512008 (2005).
10. D. Adamova, *et al.* Phys. Rev. Lett. **90** (2003) 022301.
11. G. Roland (for the PHOBOS Collaboration) nucl-ex/0510042 (2005).
12. S. Manly (for the PHOBOS Collaboration) nucl-ex/0510031 (2005).
13. A. Tounsi, A. Mischke and K. Redlich, Nucl. Phys. **A715** (2003) 565.
14. H. Caines nucl-ex/0608008 (2006).
15. E. Andersen *et al.* (WA97 Collaboration), Phys. Lett. **449** (1999) 401 and F. Antinori (for the WA97/NA57 Collaboration), Nucl. Physics **A698** (2002) 118.
16. O. Barannik (for the STAR Collaboration) J. Phys. G **31** (2005) S93.
17. B.B. Back, *et al.*, Nucl. Phys. **A757** (2005) 28.
18. J. Adams *et al.* (STAR Collaboration) Phys. Rev. Lett. **92** (2004) 112301.
19. S. Adler *et al.* (PHENIX Collaboration) Phys. Rev. **C 69** (2004) 034909.
20. J. Adams *et al.* (STAR Collaboration) nucl-ex/0604019 (2006).